Redshift of the excited state due to a nondegenerate biexciton in self-organized quantum dots

K. Kim,[1,a)] T. B. Norris,[2] and U. Hohenester[3]
[1]*School of Mechanical Engineering, Yonsei University, 134 Shinchon-dong, Seodaemun-gu, Seoul 120-749, Republic of Korea*
[2]*Department of Electrical Engineering and Computer Science, The University of Michigan, 2200 Bonisteel Blvd., Ann Arbor, Michigan 48109-2099, USA*
[3]*Institut für Physik, Karl-Franzens-Universität Graz Universitätsplatz 5, 8010 Graz, Austria*

(Received 19 October 2007; accepted 29 February 2008; published online 2 June 2008)

Using femtosecond differential transmission spectroscopy, we observed a "nondegenerate" biexciton, consisting of an electron-hole pair in the dot ground state and an electron-hole pair in the excited state, in InGaAs self-organized quantum dots. We resonantly pumped the ground state transition in the quantum dots and observed an induced resonance in the probe differential transmission spectrum near the first excited-state transition, which we attribute to the formation of a nondegenerate biexciton state. The binding energy of 15 meV does not change with excitation power, thus reflecting a genuine feature of few-particle states. Our theoretical model calculations show good agreement with these experimental results. When a prepulse is used to generate a population inversion in the quantum dots, we also observed the effects of nondegenerate biexcitonic correlations in differential transmission. © *2008 American Institute of Physics*.
[DOI: 10.1063/1.2913496]

I. INTRODUCTION

Semiconductor quantum dots (QDs) of nanometer size are of particular interest since carriers are confined within dimensions smaller than or comparable to the bulk exciton Bohr radius. This confinement in three dimensions results in a characteristic discrete energy spectrum and atomiclike carrier density of states.[1] There have been extensive efforts to fabricate and study QDs because of their potential device applications as efficient lasers and nonlinear optical materials, as well as by the interest in the experimental studies of quantum mechanical phenomena in artificial atoms. The presence of few confined carriers in such a small volume gives rise to correlated few carrier multiplexes, which might be unstable and breakup into spatially separated elements in higher dimensional systems such as quantum wells. A "ground state" biexciton, i.e., the ground state (GS) of a carrier complex with two electron-hole pairs with opposite spin orientations, has been investigated in semiconductor quantum dots.[2–8] As biexciton formation has potential applications for quantum computing and optical switching, there has been much research to characterize and understand its nature.[9–12]

In this work, we report the observation of a "nondegenerate" biexciton of two electron-hole pairs in the respective ground and excited states (ES) in InGaAs self-organized QDs using femtosecond white light spectroscopy. We resonantly pumped the GS and observed an induced resonance in the probe differential transmission (DT) spectrum, which shows the "binding energy" of the nondegenerate biexciton as 15 meV. This resonance energy is not influenced by a further increase in carrier density, thus reflecting a genuine feature of few-particle quantum dot states. Theoretical model calculations show good agreement with our experimental measurements. In an inverted QD system, we also observed the effects of nondegenerate biexciton correlations.

Our QD sample and experimental techniques are described in Sec. II, and the experimentally observed induced resonances are discussed in Sec. III. The DT/*T*s of possible biexciton formations (i.e., a ground state and a nondegenerate biexcitons) are calculated in Sec. IV using the density matrix formalism. We discuss the experimental observations and theoretical model calculations of a nondegenerate biexciton in the absorption and gain regimes in Sec. V, and conclude in Sec. VI.

II. EXPERIMENT

The $In_{0.4}Ga_{0.6}As$ QD sample used in this work is an undoped heterostructure[13] with four layers of $In_{0.4}Ga_{0.6}As$ quantum dots, separated by 2.5 nm GaAs barriers, grown by molecular beam epitaxy. These layers are sandwiched between two 0.1 μm-thick GaAs layers and two outer 0.5 μm $Al_{0.3}Ga_{0.7}As$ carrier confinement layers. The structures are grown on (001) semi-insulating GaAs substrates which are subsequently removed through selective etching to enable DT measurements. The $In_{0.4}Ga_{0.6}As$ dots are grown at 520 °C while the rest of the sample is grown at 620 °C. Cross-sectional transmission electron microscopy shows that the dots are pyramidal in shape with a base dimension of 14 nm and a height of 7 nm. Atomic force microscopy scans reveal a dot density of 5×10^{10} cm^{-2} per layer.

Band structure calculations of individual QDs based on an eight-band $\mathbf{k}\cdot\mathbf{p}$ formalism predict several confined electron and hole levels.[14] The interband transition probabilities are high only for transitions between electron and hole levels

a)Electronic mail: kks@yonsei.ac.kr.

of the same quantum number. These discrete levels are inhomogeneously broadened due to the size fluctuation of the dots. The first excited level in each dot has a twofold degeneracy due to the symmetry of the dot geometry, in addition to the double spin degeneracy.[15] At low temperature, the ES interband transition $E2H2$ is around 920 nm, and the GS transition $E1H1$ is centered at 970 nm.

Femtosecond three-pulse (or two-pulse) white-light pump and probe DT spectroscopy is performed for the gain (or absorption) regime measurement using the 85 fs, 3.5 μJ, 250 kHz Ti:sapphire regenerative amplifier system.[16] Carriers are injected by optically pumping the GaAs barrier region (800 nm, "gain pulse") to establish a population inversion in QDs; the intensity of the gain pulse is adjusted so that the dots can be in the absorption or gain regime. Tunable pump and probe pulses are generated by spectrally filtering two single-filament white-light sources; a 10 nm bandwidth "pump pulse" is tuned to resonantly deplete (or generate) electron-hole pairs in the ground or excited state by stimulated emission (or absorption) in the gain (or absorption) regime. The pump pulse is fixed after a 20 ps delay with respect to the gain pulse because the carrier population in QD is saturated at this time. The depletion (generation) of carriers by the pump pulse in the ground or excited state gives rise to a negative (positive) DT signal; this sign-flip of the DT signal is the critical indication of gain in the QDs. We used the piezoelectric shaker in the pump beam line to remove coherent interference pattern between pump and probe pulse. Cross-linear polarizations for pump (vertical) and probe (horizontal) beams are used to increase the signal-to-noise ratio by reducing the scattered pump light with an analyzing polarizer in front of the spectrometer.

A broadband white-light probe measures the DT spectrum as a function of pump-probe delay. We select the spectral band between 880 and 1030 nm with an RG850 Schott filter and use a prism pair to compensate for group velocity dispersion to limit the relative group delay to about 50 fs within this spectral range. Spectral components shorter than 850 nm in the probe are removed by a mask in the prism-pair arm to prevent any carrier generation in the GaAs barriers by the probe pulse. The pump pulse is mechanically chopped at 6 kHz, and the DT signal is measured using a lock-in amplifier; the probe DT is plotted as a function of delay following the pump pulse. The three pulses are focused using a 7.5 cm achromatic lens on the QD sample at near normal incidence.

III. OBSERVATION OF AN INDUCED RESONANCE

Femtosecond two-pulse pump-probe DT measurements are carried out by resonantly pumping the GS of the QDs and probing with broadband spectrum. A gain pulse was not introduced in this experiment. DT/T spectra at different probe delay times at $T=8$ K are shown in Fig. 1(a). Near time zero, the pump pulse generates a positive DT (induced transmission) spectrum centered at the pump wavelength (970 nm); this is the usual spectral hole burning due to the carrier population injected into the $E1H1$ QD level. Immediately after the pump pulse, a broad positive DT spectrum around the excited state and a narrow negative DT dip at 942 nm are

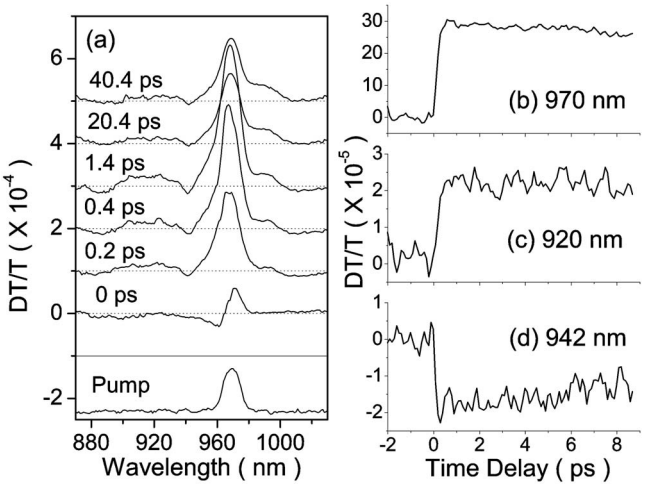

FIG. 1. (a) DT/T spectra measured with a 970 nm pump and a broadband white-light probe vs probe delay, and DT time scans measured with 970 nm pump and probe of (b) 970, (c) 920, and (d) 942 nm at $T=8$ K.

observed. Figures 1(b) and 1(c) show the time-resolved pump-probe DT dynamics for the GS (970 nm) and ES (920 nm) transitions when we resonantly pumped the GS. The time-resolved pump-probe scan of the negative DT at 942 nm is shown in Fig. 1(d). These data indicate that the induced absorption signals at 942 nm rises with the integral of the pump pulse, exactly as for the induced transmission signals on the GS and ES. This implies that these spectral features arise from the ground state population, rather than from thermal excitation of GS carriers into the excited state. The peak amplitudes of spectral holes generated in GS are measured to be linearly proportional to the power of resonant pump pulse. This linearity signifies that our observation is related to the nonlinear third-order susceptibility $\chi^{(3)}$.

IV. BIEXCITON FORMATION

After a resonant pump generates an exciton in the GS, a broadband probe can generate another exciton in the ground or excited state to form a biexciton. The binding energy of a biexciton may generate the induced resonance of Fig. 1(a). In the following, we adopt the usual assumption that biexcitons inside QDs in strong confinement regime have a dominant single-particle character and can thus be labeled in terms of GS and ES exciton states. As the total number of states in the ground state transition is known to be two including spin degeneracy, a biexciton composed of two GS excitons (degenerate) requires antiparallel spin states. In addition to this ground state (2GS) biexciton, the excited nondegenerate biexciton state could be responsible for the negative dip at 942 nm (1.316 eV) observed in our two-pulse experiment. To clear this ambiguity, we calculated DT/T spectra using the density matrix formalism for a ground state and a nondegenerate biexcitons, respectively.[17,18]

A. A ground state biexciton

When there is no coupling between the GS and ES exciton formations, the ES or GS exciton formation behaves independently of each other. In this case, a ground state biex-

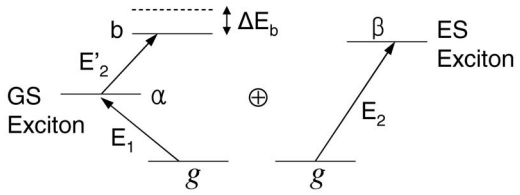

FIG. 2. A diagram showing the formation of a ground state biexciton with binding energy ΔE_b. E_1 and E_2 refer to the pump and probe pulse, respectively.

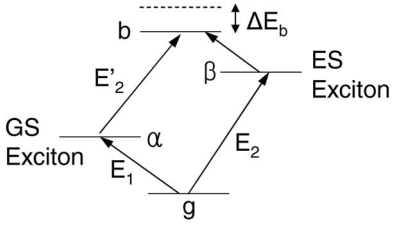

FIG. 3. A diagram showing the formation of a nondegenerate biexciton with binding energy ΔE_b. E_1 and E_2 refer to the pump and probe pulse, respectively.

citon state (2GS) with a binding energy ΔE_b can be optically induced through a process schematically depicted in Fig. 2. As there is no direct optical transition from the ES exciton to the ground state biexciton, we can restrict our analysis to the following states:

$$|g\rangle = |0\rangle,$$

$$|\alpha\rangle = |\alpha\rangle,$$

$$|b_\alpha\rangle \simeq |2\alpha\rangle,$$

$$|\beta\rangle = |\beta\rangle.$$

Here $|g\rangle$ is the semiconductor vacuum (no electron-hole pairs present), and $|\alpha\rangle$ ($|\beta\rangle$) is the single-exciton state in the GS (ES). $|b\rangle$ is the ground state biexciton state of 2GS excitons with a binding energy. The third order susceptibilities after the pump (E_1, spectrally narrow part of GS) and probe (E_2, broadband including GS and ES) are calculated using the density matrix formalism

$$\rho_{\alpha g}^{(3)} \simeq \frac{iN_0}{8\hbar^3}(4[\mu_{\alpha \mathbf{g}} \cdot \mathbf{E}_2][\mu_{\alpha \mathbf{g}}^* \cdot \mathbf{E}_1^*][\mu_{\alpha \mathbf{g}} \cdot \mathbf{E}_1]), \tag{1}$$

$$\rho_{b\alpha}^{(3)} \simeq -\frac{iN_0}{8\hbar^3}(2[\mu_{\mathbf{b}\alpha} \cdot \mathbf{E}_2][\mu_{\alpha \mathbf{g}}^* \cdot \mathbf{E}_1^*][\mu_{\alpha \mathbf{g}} \cdot \mathbf{E}_1]). \tag{2}$$

The DT/T signal is derived by including the spin degeneracies of 2 for both $P_{\alpha g}^{(3)}$ and $P_{b\alpha}^{(3)}$ and accounting for the inhomogeneous broadening $g^{(0)}$,

$$\frac{DT}{T} \propto \frac{k_2 L N_0^2}{2\hbar^3 |E_2|^2}\{C_d E_2^2[g(\omega - \omega_{g,0} + \Delta\omega_g)] + D_d E_2^2[g^{(0)}(\omega - \omega_{g,0})]\}, \tag{3}$$

$$C_d = -\mu_{b\alpha}^2 \mu_{\alpha g}^2 E_1^2, \tag{4}$$

$$D_d = 2\mu_{\alpha g}^2 \mu_{\alpha g}^2 E_1^2. \tag{5}$$

Here $\omega_{g,0}$ is the GS exciton energy, and $\Delta\omega_g (=\Delta E_b/\hbar)$ is the redshift due to the biexciton binding. $g^{(0)}(g)$ is a Gaussian distribution function which accounts for the inhomogeneous broadening of the GS exciton (biexciton). After a resonant pump at GS, an induced transmission of probe in GS is described as positive D_d and an induced absorption due to the binding energy of a ground state biexciton as negative C_d.

As the total number of states in GS is two for a single dot, a ground state biexciton requires antiparallel spin states which usually has a redshift of GS energy. In addition, our sample has four layers of QDs with 2.5 nm thick barriers, and interdot electronic tunneling in vertically coupled layers may generate minibands of eight total states in the GS.[19] In this case, a ground state biexciton may be allowed as parallel spin states, and the blueshift of GS energy may generate a negative DT/T dip between GS and ES as observed in Fig. 1(a). However, no positive DT is expected at the excited state energy for a ground state biexciton.

B. A nondegenerate biexciton

A nondegenerate biexciton (1GS+1ES) with a binding energy ΔE_b can be optically generated according to the process shown in Fig. 3. To analyze this process, we consider the following states:

$$|g\rangle = |0\rangle|0\rangle,$$

$$|\alpha\rangle = |\alpha\rangle|0\rangle,$$

$$|\beta\rangle = |0\rangle|\beta\rangle,$$

$$|b\rangle \simeq |\alpha\rangle|\beta\rangle.$$

$|g\rangle$ is the semiconductor vacuum, $|\alpha\rangle$ ($|\beta\rangle$) is a single exciton state in the GS (ES), and $|b\rangle$ is the nondegenerate biexciton state of 1GS+1ES. The third order susceptibilities after the pump (E_1, spectrally narrow part of GS) and probe (E_2, broadband including GS and ES) are calculated again using the density matrix formalism

$$\rho_{\alpha g}^{(3)} \simeq \frac{iN_0}{8\hbar^3}(4[\mu_{\alpha \mathbf{g}} \cdot \mathbf{E}_2][\mu_{\alpha \mathbf{g}}^* \cdot \mathbf{E}_1^*][\mu_{\alpha \mathbf{g}} \cdot \mathbf{E}_1]), \tag{6}$$

$$\rho_{b\alpha}^{(3)} \simeq -\frac{iN_0}{8\hbar^3}(2[\mu_{\mathbf{b}\alpha} \cdot \mathbf{E}_2][\mu_{\alpha \mathbf{g}}^* \cdot \mathbf{E}_1^*][\mu_{\alpha \mathbf{g}} \cdot \mathbf{E}_1]), \tag{7}$$

$$\rho_{\beta g}^{(3)} \simeq \frac{iN_0}{8\hbar^3}(2[\mu_{\beta \mathbf{g}} \cdot \mathbf{E}_2][\mu_{\alpha \mathbf{g}}^* \cdot \mathbf{E}_1^*][\mu_{\alpha \mathbf{g}} \cdot \mathbf{E}_1]), \tag{8}$$

$$\rho_{b\beta}^{(3)} \simeq 0. \tag{9}$$

The DT/T signal is derived by including the contributions from inhomogeneous broadening and the spin degeneracies, i.e., 2, 4, and 4 for $P_{\alpha g}^{(3)}$, $P_{b\alpha}^{(3)}$, and $P_{\beta g}^{(3)}$, respectively,

$$\frac{\mathrm{DT}}{T} \propto \frac{k_2 L N_0^2}{\hbar^3 |E_2|^2}\{B_{\mathrm{nd}} E_2^2[g^{(0)}(\omega - \omega_{e,0})] + C_{\mathrm{nd}} E_2^2[g(\omega - \omega_{e,0} + \Delta\omega_e)] + D_{\mathrm{nd}} E_2^2[g^{(0)}(\omega - \omega_{g,0})]\}, \tag{10}$$

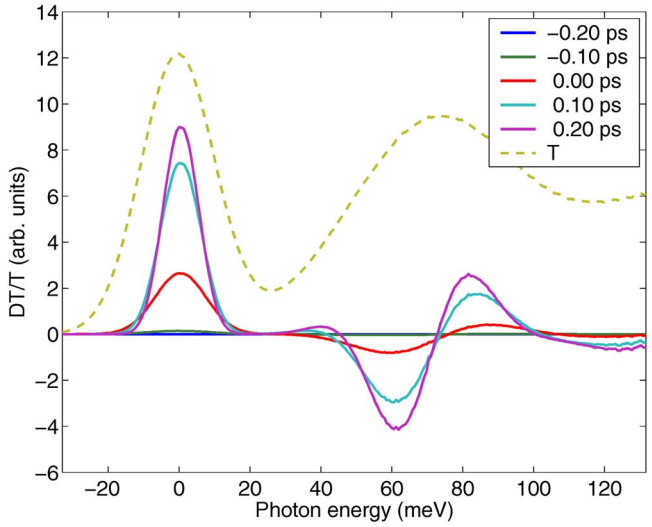

FIG. 4. (Color online) Theoretical calculation of DT/T for a parabolic and boxlike QD including the nondegenerate biexciton binding energy.

$$B_{\mathrm{nd}} = \mu_{\beta g}^2 \mu_{\alpha g}^2 E_1^2, \tag{11}$$

$$C_{\mathrm{nd}} = -\mu_{b\alpha}^2 \mu_{\alpha g}^2 E_1^2, \tag{12}$$

$$D_{\mathrm{nd}} = \mu_{\alpha g}^2 \mu_{\alpha g}^2 E_1^2. \tag{13}$$

E_1 (E_2) is the electric field of pump (probe) pulse, and E_2 covers broadband including GS and ES while E_1 covers just a narrow part of GS bandwidth. $\omega_{e,0}$ is the ES exciton energy, and $\Delta\omega_e(=\Delta E_b/\hbar)$ is the ES redshift of the nondegenerate biexciton. After a resonant pump at GS, induced transmissions of probe in GS and ES are described as positive D_{nd} and B_{nd}. Here a negative dip of DT/T between ES and GS is expected because of the binding energy of a nondegenerate biexciton, as described by the coefficient C_{nd} in Eq. (12). A positive DT at ES is also expected as described by B_{nd}.

V. OBSERVATION OF A NONDEGENERATE BIEXCITON

A negative DT between the GS and the ES is predicted in both cases of a ground state and a nondegenerate biexcitons. However, a positive DT in the excited state is not expected for the ground state biexciton but only for the nondegenerate biexciton. This clarifies that the induced resonance which we observed is from the nondegenerate biexciton.

A. Observation in the absorption regime

Figure 4 shows the results of calculated DT spectra adopting parameters of prototypical quantum dot states, i.e., material parameters for InGaAs dots and a parabolic confinement for electrons and holes (for details see Ref. 20 and the discussion later). The DT spectra at different delay times clearly exhibit a negative dip at a photon excess energy of ≈60 meV associated to the formation of a nondegenerate biexciton. Although these results can clearly reproduce all the essential features of our experiments, a more careful comparison of theory and experiment shows that our calculations somewhat overestimate the negative dip in the spectra. To inquire into these problems, we additionally performed a fitting of the coefficients B_{nd}, C_{nd}, C_d, D_{nd}, and D_d of Eqs. (3) and (10) to reproduce the observed DT spectra. These fittings and a discussion of differences to our model calculations in Fig. 4 will be presented in the following.

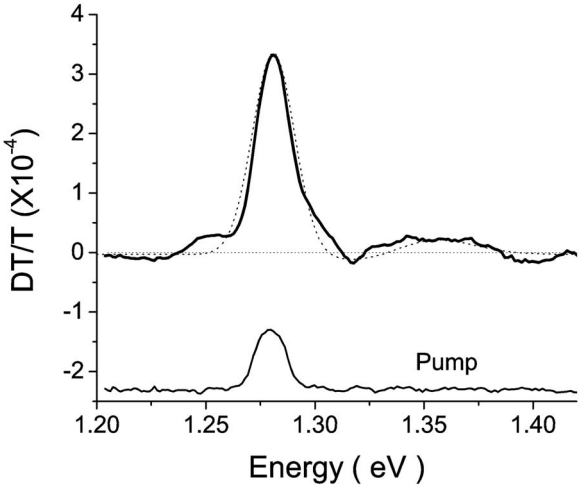

FIG. 5. Two-pulse experimental data as well as data fitting with 970 nm (GS) pump and broadband probe pulses for QDs in the absorption regime.

The dotted line in Fig. 5 is the fitting of spectral DT/T data using Eq. (10). The ES energy redshift due to the formation of a nondegenerate biexciton is obtained as 15 meV. The resonant pump at the GS energy generates a GS exciton in the dots of different size inside an energy window of 19.2 meV (corresponding to the bandwidth of the pump pulse) centered around 1.28 eV. The energy gaps between GS and ES are also different in different size dots which are the origin of inhomogeneous broadening of QD absorption spectrum. This difference of energy gaps between GS and ES makes the ES bandwidth broader than the GS bandwidth. Therefore, inhomogeneous broadening is included in the ES spectral hole of Fig. 5. The ES bandwidth is observed to be 40.1 meV and smaller than the total bandwidth of inhomogeneous broadening (52.8 meV) from the barrier-pumped measurement which we also performed for the same QDs. Since the bandwidth of the ES transition is twice of the GS transition's bandwidth, it reduces the peak amplitude of ES by 1/2 because the carrier populations are represented by the DT/T areas rather than the peak amplitudes. The contributions from spatial and spin degeneracies of states are also included in the DT/T formulation in Eq. (10). Including the effects of degeneracy and bandwidth broadening, the ratio of coefficients B_{nd}, C_{nd}, and D_{nd} is approximately 1:1:4 from our measurement, which may be from the effect of QD ensemble measurement rather than a single dot, the polarization difference between the ES and the GS transitions, and/or the tunneling interactions between vertically neighboring QDs.

We additionally performed model calculations to estimate the biexcitonic redshift ΔE_b. We adopt the framework presented in Ref. 20, where we computed few-particle spectra for $In_xGa_{1-x}As$ dots within the envelope-function and effective-mass approximations and obtained good agreement with experiment. More specifically, we assume a 2:1 ratio between electron and hole single-particle splittings[13] and a

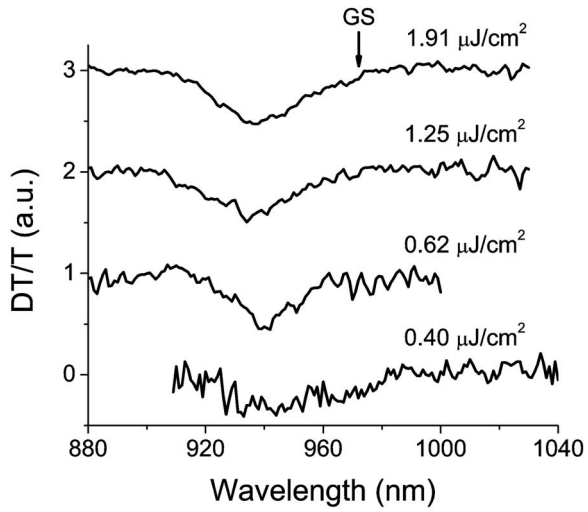

FIG. 6. DT/T spectra measured with a 970 nm (GS) pump and a broadband white-light probe in $In_{0.4}Ga_{0.6}As$ QD vs the carrier density in QDs at $T=10$ K. Carriers are optically injected into QDs using a prepulse (gain pulse) before the pump and probe pulses. Our pump pulse is 20 ps after the gain pulse, and the probe pulse is ~3 ps after the pump pulse.

20% stronger hole confinement due to the heavier hole mass and possible piezoelectric fields[20] and compute the single-exciton and biexciton states for different dot sizes within a direct-diagonalization approach accounting for all Coulomb interactions among the photoexcited carriers.[21] Results of these calculations reveal a biexcitonic redshift ΔE_b of the order of 10 meV which depends relatively weakly on dot size. When we further increase the carrier density in the QD, our model calculations also show that the transition from 2GS to (2GS+ES) is almost at the same energy as the transition from 1GS to (1GS+1ES) because of the Coulomb correlation effects of the few-particle system. In Sec. V B, we experimentally measured the ES energy in higher carrier density and the results give good agreement with our model calculations.

B. Observation in the gain regime

The behavior of the ES energy in even higher carrier density is very interesting because it is critical for the QD laser behavior. In order to measure the ES energy in higher carrier density, we used the three-pulse pump-probe technique as described in Sec. II. We resonantly pumped the GS and changed the carrier density in QD by adjusting the gain pulse intensity. The carriers in the ES are the main reservoir for the gain recovery of the carrier depletion in the GS, and the intradot relaxation from ES to GS is as fast as 130 fs.[16] The negative hole burning of ES after the gain recovery of GS versus the carrier density in QD at $T=10$ K are plotted in Fig. 6. The probe pulse is ~3 ps after the pump pulse. In the case of 0.40 $\mu J/cm^2$ fluence density, the depleted GS is not totally recovered because the carrier number in ES is not enough. These data show that the ES energy does not change after the redshift due to the formation of a nondegenerate biexciton even though we further increase the mean carrier density in QDs. And these results give good agreement with our model calculations described in Sec. V A.

The effects of a nondegenerate biexciton may be observed in inverted QD system using the three-pulse pump-probe technique. If we establish a population inversion in both GS and ES of QD by photoinjection of carriers in barriers, the initial QD population is $\rho_{bb}^{(0)}=N_0$ because of the nondegenerate biexciton formations. The third order susceptibilities after pump (E_1, spectrally narrow part of redshifted ES) and probe (E_2, broadband including GS and ES) are calculated with the density matrix formalism

$$\rho_{b\alpha}^{(3)} \simeq -\frac{iN_0}{8\hbar^3}(4[\mu_{\mathbf{b}\alpha}\cdot\mathbf{E}_2][\mu_{\mathbf{b}\alpha}^*\cdot\mathbf{E}_1^*][\mu_{\mathbf{b}\alpha}\cdot\mathbf{E}_1]), \tag{14}$$

$$\rho_{\alpha g}^{(3)} \simeq \frac{iN_0}{8\hbar^3}(2[\mu_{\alpha\mathbf{g}}\cdot\mathbf{E}_2][\mu_{\mathbf{b}\alpha}^*\cdot\mathbf{E}_1^*][\mu_{\mathbf{b}\alpha}\cdot\mathbf{E}_1]), \tag{15}$$

$$\rho_{b\beta}^{(3)} \simeq -\frac{iN_0}{8\hbar^3}(2[\mu_{\mathbf{b}\beta}\cdot\mathbf{E}_2][\mu_{\mathbf{b}\alpha}^*\cdot\mathbf{E}_1^*][\mu_{\mathbf{b}\alpha}\cdot\mathbf{E}_1]), \tag{16}$$

$$\rho_{\beta g}^{(3)} \simeq 0. \tag{17}$$

The DT/T signal is again derived after including the contributions from spatial and spin degeneracies of states as 4, 2, and 4 for $P_{b\alpha}^{(3)}$, $P_{\alpha g}^{(3)}$, and $P_{b\beta}^{(3)}$, respectively,

$$\frac{\mathrm{DT}}{T} \propto \frac{k_2 L N_0^2}{4\hbar^3|E_2|^2}\{B_g E_2^2[g^{(0)}(\omega-\omega_{g,0})] + C_g E_2^2[g(\omega-\omega_{g,0} + \Delta\omega_g)] + D_g E_2^2[g^{(0)}(\omega-\omega_{e,0})]\}, \tag{18}$$

$$B_g = \mu_{g\alpha}^2\mu_{b\alpha}^2 E_1^2, \tag{19}$$

$$C_g = -2\mu_{b\beta}^2\mu_{b\alpha}^2 E_1^2, \tag{20}$$

$$D_g = -4\mu_{b\alpha}^2\mu_{b\alpha}^2 E_1^2. \tag{21}$$

E_1 (E_2) is the electric field of the pump (probe) pulse, and E_2 covers both the GS and ES transition energies while E_1 covers just a narrow part of the redshifted ES bandwidth. $\omega_{g,0}$ is the GS energy level when there is no exciton in the ES, and $\Delta\omega_g(=\Delta E_b/\hbar)$ is the GS energy level redshift due to an exciton in ES. $g^{(0)}$ is the Gaussian distribution function of QDs which have carriers in GS including inhomogeneous broadening effect when there is no exciton in ES, and g is the distribution function when there is an exciton in ES. Coefficient D_g describes a spectral hole burning (negative DT/T) in ES generated by the carrier depletion due to the stimulated emission with pump pulse in an inverted QD system. Coefficients B_g and C_g describes the effects of a nondegenerate biexciton and generate a positive DT/T in GS and a negative DT/T in the red side of GS, respectively. In an inverted QD system, a negative DT recovers rapidly due to the ultrafast gain recovery from higher energy states while a positive DT lasts.[16] Especially in low temperature, the GS is totally filled with carriers before the ES is inverted and the positive DT in GS is not expected from phonon-mediated process or gain recovery dynamics when we resonantly pump the ES.

We established a population inversion to obtain gain in the GS and ES with a gain pulse of 800 nm at $t=-20$ ps. The fluence of gain pulse is 2.04 $\mu J/cm^2$ and corresponds to 6.2

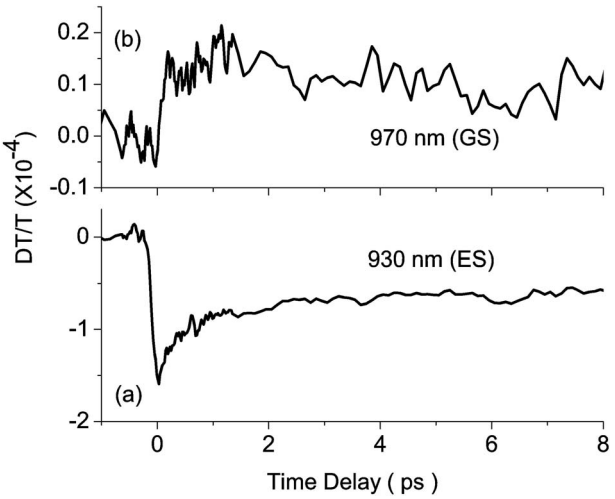

FIG. 7. DT time scans at $T=10$ K measured with 930 nm (ES) resonant pump and (a) 930 nm (ES) probe and (b) 970 nm (GS) probe for gain pulse fluence of 2.04 $\mu J/cm^2$ (6.2 electron-hole pairs per a dot).

electron-hole pairs per a dot. A pump pulse at 930 nm depletes the carriers in ES via stimulated emission at $T=10$ K. The temporal evolution of the excited state gain recovery is shown in Fig. 7(a) and can be explained by coefficient D_g in Eq. (21). Our spectrally resolved data indicate that higher energy states are the carrier reservoir for the ultrafast gain recovery of ES as discussed in Ref. 16. If we measure the ground state dynamics along with the carrier depletion and gain recovery of ES, we obtain a positive DT in the GS at 970 nm, as shown in Fig. 7(b), as expected by a coefficient B_g in Eq. (19). The observation of this positive DT/T signal in GS indicates the effect of a nondegenerate biexciton correlation.

VI. CONCLUSION

By resonantly pumping the ground state of QDs, we observed instantaneous positive DT at ES and a negative dip of DT between GS and ES in the absorption regime. The negative dip is an induced absorption generated by a nondegenerate biexciton (1GS+1ES). The binding energy of a nondegenerate biexciton (1GS+1ES) is experimentally observed to be 15 meV, and this redshifted ES energy does not change in higher carrier density in QDs. Our theoretical model calculations show good agreement with these experimental measurements. We resonantly pumped the ES in inverted QDs using a gain pulse to establish a population inversion in GS and ES, and the effects of a nondegenerate biexciton correlation are also observed. This nondegenerate biexciton can be used for nondegenerate coherent control and optical switching.

ACKNOWLEDGMENTS

We thank Professor Bhattacharya for the supply of QD samples. This study was supported by a grant from the National R & D Program for Cancer Control, Ministry of Health & Welfare, Republic of Korea (0720170), by the Bio R & D program through the Korea Science and Engineering Foundation funded by the Ministry of Science & Technology (KOSEF 2007-8-1158), and by a Korea Research Foundation Grant provided by the Korean Government (MOEHRD, Basic Research Promotion Fund) (KRF-2007-331-C00121).

[1] D. Bimberg, M. Grundmann, and N. N. Ledentsov, *Quantum Dot Heterostructures* (Wiley, Chichester, 1998).
[2] Y. Z. Hu, S. W. Koch, M. Lindberg, N. Peyghambarian, E. L. Pollock, and F. F. Abraham, Phys. Rev. Lett. **64**, 1805 (1990).
[3] K. I. Kang, A. D. Kepner, S. V. Gaponenko, S. W. Koch, Y. Z. Hu, and N. Peyghambarian, Phys. Rev. B **48**, 15449 (1993).
[4] E. Dekel, D. Gershoni, E. Ehrenfreund, J. M. Garcia, and P. M. Petroff, Phys. Rev. B **61**, 11009 (2000).
[5] E. Dekel, D. Gershoni, E. Ehrenfreund, D. Spektor, J. M. Garcia, and P. M. Petroff, Phys. Rev. Lett. **80**, 4991 (1998).
[6] R. Levy, L. Mager, P. Gilliot, and B. Hönerlage, Phys. Rev. B **44**, 11286 (1991).
[7] Y. Z. Hu, M. Lindberg, and S. W. Koch, Phys. Rev. B **42**, 1713 (1990).
[8] T. Takagahara, Phys. Rev. B **39**, 10206 (1989).
[9] E. Biolatti, R. C. Iotti, P. Zanardi, and F. Rossi, Phys. Rev. Lett. **85**, 5647 (2000).
[10] P. Chen, C. Piermarocchi, and L. J. Sham, Phys. Rev. Lett. **87**, 067401 (2001).
[11] F. Troiani, U. Hohenester, and E. Molinari, Phys. Rev. B **62**, R2263 (2000).
[12] P. Zanardi and F. Rossi, Phys. Rev. Lett. **81**, 4752 (1998).
[13] J. Urayama, T. B. Norris, J. Singh, and P. Bhattacharya, Phys. Rev. Lett. **86**, 4930 (2001).
[14] H. Jiang and J. Singh, Phys. Rev. B **56**, 4696 (1997).
[15] K. Kim, T. B. Norris, S. Ghosh, J. Singh, and P. Bhattacharya, Appl. Phys. Lett. **82**, 1959 (2003).
[16] K. Kim, J. Urayama, T. B. Norris, J. Singh, J. Phillips, and P. Bhattacharya, Appl. Phys. Lett. **81**, 670 (2002).
[17] I. M. Beterov and V. P. Chebotaev, Prog. Quantum Electron. **3**, 1 (1974).
[18] M. O. Scully and M. S. Zubairy, *Quantum Optics* (Cambridge University Press, Cambridge, 1997).
[19] J. Urayama, T. B. Norris, B. Kochman, J. Singh, and P. Bhattacharya, Appl. Phys. Lett. **76**, 2394 (2000).
[20] F. Findeis, M. Baier, A. Zrenner, M. Bichler, G. Abstreiter, U. Hohenester, and E. Molinari, Phys. Rev. B **63**, 121309(R) (2001).
[21] M. Rontani, F. Troiani, U. Hohenester, and E. Molinari, Solid State Commun. **119**, 309 (2001).